

1S_0 Pairing in Neutron Matter

H.-H. Fan^{1,2} · E. Krotscheck^{1,2}  · J. W. Clark^{3,4}

Received: 21 July 2017 / Accepted: 18 September 2017 / Published online: 2 October 2017
© Springer Science+Business Media, LLC 2017

Abstract We report calculations of the superfluid pairing gap in neutron matter for the 1S_0 components of the Reid soft-core V_6 and the Argonne V'_4 two-nucleon interactions. Ground-state calculations have been carried out using the central part of the operator-basis representation of these interactions to determine optimal Jastrow–Feenberg correlations and corresponding effective pairing interactions within the correlated basis formalism, the required matrix elements in the correlated basis being evaluated by Fermi hypernetted-chain (FHNC) techniques. Different implementations of the Fermi hypernetted-chain Euler–Lagrange (FHNC-EL) method agree at the percent level up to nuclear matter saturation density. For the assumed interactions, which are realistic within the low density range involved in 1S_0 neutron pairing, we did not find a dimerization instability arising from divergence of the in-medium scattering length, as was reported recently for simple square-well and Lennard–Jones potential models (Fan et al. in Phys Rev A 92:023640, 2015).

Keywords Superfluidity · Quantum fluids · Neutron matter

✉ E. Krotscheck
eckhardk@buffalo.edu

¹ Department of Physics, University at Buffalo SUNY, Buffalo, NY 14260, USA

² Institut für Theoretische Physik, Johannes Kepler Universität, 4040 Linz, Austria

³ Department of Physics and McDonnell Center for the Space Sciences, Washington University, St. Louis, MO 63130, USA

⁴ Centro de Investigação em Matemática e Aplicações, University of Madeira, 9020-105 Funchal, Madeira, Portugal

1 Introduction

1.1 Adaptation of BCS Theory to Nuclear Systems

The nature and role of fermionic pairing and superfluidity in nuclei and nuclear matter became a subject of great interest shortly after publication of the landmark paper by Bardeen, Cooper, and Schrieffer (BCS) establishing the physical basis of superconductivity in metals [1, 2]. Bohr et al. [3] were quick to recognize implications of this development for a deeper understanding of nuclear phenomena, relating it to evidence for a characteristic energy gap between the ground state and the first intrinsic excitation in a certain class of nuclei.

Concurrently, there was growing interest among nuclear theorists in what could be learned from the quantum many-body problem of infinite nuclear matter composed of nucleons interacting through the best nucleon–nucleon (NN) potentials available at the time. Cooper et al. [4] (CMS) were the first to apply BCS theory to such a system. They encountered two obstacles when attempting to solve the BCS equation for the superfluid energy gap $\Delta_{\mathbf{k}}$ as a function of momentum \mathbf{k} .

To understand what they faced, it is necessary to consider the BCS gap equation, written in the generic form

$$\Delta_{\mathbf{k}} = - \sum_{\mathbf{k}'} P_{\mathbf{k},\mathbf{k}'} \frac{\Delta_{\mathbf{k}'}}{2E_{\mathbf{k}'}} \tag{1}$$

where $P_{\mathbf{k},\mathbf{k}'} = \langle \mathbf{k} \uparrow, -\mathbf{k} \downarrow | V(12) | \mathbf{k}' \uparrow, -\mathbf{k}' \downarrow \rangle$ defines the pairing matrix elements of the bare two-body potential $v(12)$, while

$$E_{\mathbf{k}} = [(e_{\mathbf{k}} - \mu)^2 + \Delta_{\mathbf{k}}^2]^{1/2} \tag{2}$$

represents the (gapped) quasiparticle energy in the superfluid state, with $e_{\mathbf{k}}$ an “appropriate” single-particle energy related to the normal state. Given the original BCS trial ground state

$$|\text{BCS}\rangle = \prod_{\mathbf{k}} \left[u_{\mathbf{k}} + v_{\mathbf{k}} a_{\mathbf{k}\uparrow}^{\dagger} a_{-\mathbf{k}\downarrow}^{\dagger} \right] |0\rangle \tag{3}$$

(but written slightly differently in terms of Bogoliubov amplitudes $u_{\mathbf{k}}$, $v_{\mathbf{k}}$ satisfying the normalizing condition $u_{\mathbf{k}}^2 + v_{\mathbf{k}}^2 = 1$), the expression (1) of the gap equation can be derived from the Euler–Lagrange variational principle following exactly the same path as in the 1957 BCS paper [1] and in Schrieffer’s book [5]. As the BCS state does not have a definite particle number, the chemical potential μ (determined from the number density) is introduced as a Lagrange parameter to accommodate the constraint that the particle number is conserved on average.

Of the two problems CMS faced in implementing BCS theory for nuclear matter, they managed to solve what appeared to be the more difficult one, and finessed the other. During this same period in the mid-to-late 1950s, it had become apparent that an

acceptable model of the NN interaction, fitted to the available NN scattering data and the deuteron, must possess a strong inner repulsion, most commonly taken to be a hard core. This precluded solving the BCS gap equation as formulated in momentum space, because the necessary pairing matrix elements $P_{\mathbf{k},\mathbf{k}'}$ of the NN potential would be undefined. However, CMS recognized that the BCS gap equation could be transformed to coordinate space to yield a nonlinear but Schrödinger-like equation for an underlying two-body problem. The analog of the wave function for the separation vector \mathbf{r} is the pairing function $\chi(\mathbf{r})$, which may also be regarded as the superfluid order parameter. Basically, $\chi(\mathbf{r})$ is the Fourier transform of the product $u_{\mathbf{k}}v_{\mathbf{k}}$ of Bogoliubov amplitudes, or equivalently of $\Delta(\mathbf{k})/2E_{\mathbf{k}}$. Therefore, the problem created by the hard core of the NN potential could be solved, for the same reason that the Schrödinger equation for a hard-sphere scattering potential has a solution.

The second problem confronting CMS was what to take for the single-particle energy $e_{\mathbf{k}}$ in the expression for $E_{\mathbf{k}}$. There is first a subtlety relating to $e_{\mathbf{k}}$ that should be exposed, for the record. The above derivation leads to the actual expression

$$e_{\mathbf{k}} = \frac{\hbar^2 k^2}{2m} + \frac{1}{2} \sum_{\mathbf{l}\sigma\sigma'} v_{\mathbf{l}}^2 \langle \mathbf{k}\sigma, \mathbf{l}\sigma' | V(12) | \mathbf{k}\sigma, \mathbf{l}\sigma' - \mathbf{l}\sigma', \mathbf{k}\sigma \rangle, \quad (4)$$

where σ and σ' are the spin projections. This contains the Fermi-surface smearing factor represented by $v_{\mathbf{l}}^2$, and hence requires a solution of the pairing problem before $e_{\mathbf{k}}$ can be evaluated. In practice, this factor is almost always replaced by the Fermi step, converting $e_{\mathbf{k}}$ to a standard Hartree–Fock single-particle energy. It is argued, in most cases safely, that this can be done because the gap $\Delta_{\mathbf{k}}$ is much smaller than the Fermi energy, thus decoupling $e_{\mathbf{k}}$ from the rest of the gap problem.

The primary issue raised by the expression (4) is not at all subtle. If the bare NN interaction contains a hard core, the Hartree–Fock matrix elements it contains are infinite; nor would the results for $e_{\mathbf{k}}$ be sensible if the interaction remains finite, but features an internal repulsion strong enough to achieve empirical saturation of nuclear matter. CMS were forced to finesse this second problem; they imposed an effective-mass spectrum $e_{\mathbf{k}} = \hbar^2 k^2 / 2m^*$. With this step, the problem was well defined and in principal soluble for $\Delta_{\mathbf{k}}$; however, for some time only the *existence* of a superfluid solution was established [6], due to the limited computational resources of that period.

In summary, the nature of the BCS theory of superfluidity is such that its application to nuclear systems is practical, in particular for the hypothetical system of infinite nuclear matter and certain nucleonic subsystems existing in neutron stars. However, due to the presence of a strong short-range repulsion in the bare NN interaction, one must make a reasonable, but ad hoc, assumption for the normal-state single-particle energy. The theory has the capacity to generate two-body correlations that can accommodate even the effects of a hard core, although the problem must then be solved in coordinate space. Solution of the problem in momentum space, i.e., the original gap equation (1), does in fact become possible if the NN interaction, even though strongly repulsive at short distance, has a Fourier transform. (For some interactions including the Reid soft-core potential [7, 8], numerical solution can present

some technical difficulty; this can be avoided by applying the separation approach developed in Ref. [9]).

Yet the status of nuclear BCS as described remains unsatisfactory for potentials with repulsive cores. This issue was naturally addressed by the introduction of Jastrow–Feenberg correlation factors [10–12]. Cluster-expansion techniques were applied to evaluate the required expectation values [13]. The corresponding gap equations were studied and procedures for their solution explored, with applications not only to isospin-symmetric nuclear matter (equal numbers of neutrons and protons) [10], but also pure neutron matter and β -stable nucleonic matter relevant to neutron-star interiors [11, 14]. In the mid-1970s, major advances in microscopic quantum many-body theory involving correlated basis functions (CBF) were made with the replacement of cluster expansions by Fermi hypernetted-chain (FHNC) diagram-resummation techniques [13, 15], facilitating accurate evaluation of expectation values and matrix elements of observables in a correlated basis and culminating in a framework for Euler–Lagrange optimization of Jastrow–Feenberg correlations. When implemented in a BCS extension, these advances have made possible the development of a rigorous correlated BCS (CBCS) theory [16] (see also Ref. [17]) that respects the U(1) symmetry-breaking aspect of the superfluid state—i.e., non-conservation of particle number. Some earlier applications of CBCS theory to nuclear systems, and especially neutron-star matter, may be found in Refs. [8, 16]. A recent in-depth study of correlations in the low-density Fermi gas [18], with emphasis on the presence of Cooper pairing and dimerization, documents the power of the Euler–Lagrange FHNC approach adopted in the present work, especially when coupled with CBF perturbation theory.

1.2 Extension of BCS Asymptotics to Structured Interactions and In-Medium Effects

Having derived the equivalent of the gap equation (1), BCS went on to simplify the pairing interaction in a way suitable for electron liquids in solids, arriving at the iconic asymptotic result

$$\Delta \simeq 2\hbar\omega_c e^{-1/\lambda} \quad (5)$$

for the value of the energy gap Δ in terms of a cutoff $\hbar\omega_c$ and the coupling constant $\lambda = |N(0)V|$ of the attractive pairing interaction V , with $N(0)$ denoting the density of states around the Fermi surface. It is important to recognize that this result, being restricted to the weak-coupling regime $\lambda \ll 1$, is not at all appropriate for nuclear problems. In nuclear systems, the bare two-body interaction is strong, and strongly non-monotonic in coordinate space. Two parameters are not sufficient to characterize the asymptotic behavior of the gap at relevant densities. See Refs. [9, 19] for extensive analysis and computational exploration of this important distinction. The latter reference includes an asymptotic study in which the pairing interaction is characterized by an additional parameter κ along with the traditional coupling constant λ and cutoff frequency ω . This “stiffness” parameter is introduced to represent a non-trivial momentum dependence of the pairing interaction $P_{\mathbf{k}\mathbf{k}'}$. Asymptotic behavior in the four quadrants ($\lambda \pm, \kappa \pm$)

is explored in Ref. [19], pointing to the existence of solutions with behavior quite distinct from the familiar relation (5), in addition to a BCS-analog.

Another asymptotic formula of special interest (and of long standing) is that of Gorkov and Melik-Barkhudarov [20] (GM),

$$\Delta_F = (4e)^{-1/3} \frac{8}{e^2} e_F e^{-1/\lambda}, \quad (6)$$

written for the zero-temperature gap rather than the critical temperature. This result was derived by field-theoretic methods in the limit of an infinitely dilute gas of interacting spin-1/2 fermions, with $\lambda = 2k_F|a_0|/\pi$. Here, a_0 is the *vacuum* scattering length, assumed to be negative, $e_F = \hbar^2 k_F^2/2m$ is the Fermi energy, m the fermion mass, and k_F the Fermi momentum. The prefactor $(4e)^{-1/3}$ is an in-medium correction for a polarization-induced interaction corresponding to exchange of virtual phonons. The same result without the GM prefactor was re-derived several times in the 1990s, basically by summing ladder diagrams for the bare interaction (see Ref. [21], where the GM prefactor is generalized to $(4e)^{\nu/3-1}$ for an arbitrary number ν of fermion species).

In the recent work previously cited [18], it has been argued [cf. Eqs. (3.25) and (3.26)] that if one has corrections of the in-medium scattering length a to the vacuum scattering length of the form

$$a = a_0 \left[1 + \alpha \frac{a_0 k_F}{\pi} + \dots \right], \quad (7)$$

it follows that

$$\Delta_F = \frac{8}{e^2} e_F \exp\left(-\frac{\alpha}{2}\right) \exp\left(\frac{\pi}{2a_0 k_F}\right). \quad (8)$$

The GM factor is just one of these corrections, which still assumes that the pairing matrix element at k_F is the same as that at $k = 0$. Removing this assumption produces yet another correction of the same kind.

The above summary of BCS asymptotics is intended to provide deep background for the present work on neutron matter at densities occurring in the inner-crust region of neutron stars, but their direct relevance is open to question. The neutron densities involved in this application are low compared to the saturation density ρ_0 of isospin-symmetric nuclear matter, which, in pure neutron matter, would correspond to a k_F value of about 1.7 fm^{-1} . We will find that 1S_0 pairing in neutron matter is strongest at somewhat less than half that value, thus at a density an order of magnitude below ρ_0 . On the other hand, given the unusually large magnitude of the neutron-neutron S -wave scattering length, $a_0 \approx -18.6 \text{ fm}$, the diluteness condition $|a_0|k_F \ll 1$ implies $k_F \ll 0.05 \text{ fm}^{-1}$, over three orders of magnitude lower in density than that of the physically relevant neutron-star environment. Naturally, the dilute-limit asymptotics do apply for the extreme low-density tail of the roughly Gaussian shape of Δ_F versus k_F in the 1S_0 neutron pairing problem considered here. The higher-density tail is more

relevant; it has been demonstrated in Ref. [9] that Δ_F dies exponentially to naught as an upper critical density is approached.

1.3 Sensitivity Issues in Optimization

The foregoing subsections of this introduction provide a rather elaborate background and motivation for the work to be presented. Another motivation is more immediate. Recently, using updated modern NN interactions, gap calculations [22] for pure neutron matter have again been performed within the simpler version of correlated BCS theory in which the ground-state energy for a Jastrow–Feenberg trial function, estimated by a truncated cluster expansion, is minimized with respect to the parameters in an assumed analytic form for the Jastrow two-body correlation function $f(r)$. The correlation function so determined is used to generate a “tamed” effective pairing interaction for calculation of a corresponding superfluid gap in the 1S_0 state.

Reference [22] presents results for the ground-state energy per particle E/N and the corresponding 1S_0 energy gap, based on the Argonne V_{18} (AV18) NN interaction [23] and two trial correlation functions with analytic forms that have been employed in earlier Jastrow–Feenberg studies of nuclear and neutron matter. The optimal ground-state energies determined for these two choices show only minor quantitative differences over the low range of densities where a significant 1S_0 gap is to be expected (peaking at about $1/8$ nuclear saturation density). The two curves obtained for the gap $\Delta_F = \Delta(k = k_F)$ at the Fermi surface, plotted versus Fermi momentum k_F , have a Gaussian appearance. In contrast to the close agreement of the E/N results for the two correlation choices, the corresponding peak values for Δ_F are found to differ by almost a factor two (with a value 1.8 MeV for the correlation function featuring an overshoot of unity versus 3.3 MeV for one that does not).

This finding could be interpreted as a reflection of the variational property that a small error of order δ in the wave function only entails an error of order δ^2 in the energy expectation value, but of order δ for other observables, with δ in this case corresponding to the difference in the choices for $f(r)$. But the situation may actually be worse for two reasons: The most immediate one is that the gap itself shows an exponential amplification of errors in the coupling strength and density of states, at least for the standard BCS case. Some results of the present investigation indicate a similar strong sensitivity of gap behavior. The second, more subtle reason, involves the convergence of cluster expansions for correlated wave functions: Typically, the contribution of an n -body diagram in the energy is amplified by a factor of n^2 in its contribution to the effective interactions needed to calculate the coupling matrix elements.

Figure 6 of the paper of Pavlou et al. [22] shows plots of Δ_F versus k_F for the AV18 interaction as obtained in almost a dozen calculations by different theoretical methods, including various versions of Monte Carlo. (Actually, this is a summary figure taken from the review by Gezerlis et al. [24] of novel superfluidity in neutron stars, with a curve calculated by Pavlou et al. superimposed.) There is a spread of a factor of six in the peak values of Δ_F , with a significant spread also in the peak densities. In view

of what has been said above, this is hardly surprising, although the calculations may differ in the inclusion of in-medium effects.

At any rate, the message from the considerations of this subsection is that it is imperative within any variational approach to seek truly optimal correlations, without resorting to simple parametrizations, and that is what Euler–Lagrange FHNC (FHNC-EL) can deliver, with minimal error.

The rest of this paper is organized as follows. Section 2 exemplifies what qualifies as a generic many-body theory, first with a brief review of the elements of the Jastrow–Feenberg theory of the normal ground state of a many-fermion system (Sect. 2.1), then with an introduction to the formalism associated with the method of correlated basis functions (CBF) (Sect. 2.2), concluding with the essentials of a coherent theory of fermion superfluidity within the CBF framework (Sect. 2.3), based on Euler–Lagrange Fermi Hypernetted-Chain optimization (FHNC-EL). In Sect. 3.1, we describe and discuss our application of two types of FHNC-EL theory to the ground-state energetics of pure neutron matter. Section 3.2 is concerned with solution of the resulting CBF gap equation for 1S_0 pairing, which incorporates the effects of the optimal Jastrow–Feenberg correlations. Results for energetics (the equation of state) and BCS pairing in CBF framework are presented and discussed for two versions of the bare NN interaction, namely the Reid soft-core V_6 potential [7] and the Argonne V'_4 interaction [25]. Well known from earlier microscopic studies of nuclear matter, these choices are quantitatively viable in the low-density regime where the 1S_0 pairing state is dominant. Only the central components of these potentials and their 1S_0 projections are needed for determination of the CBF pairing matrix elements, in contrast to the case of the full Argonne V_{18} interaction [23]. (Note that Argonne V'_4 is central by construction and we use only the V_4 part of the Reid potential, i.e., its tensor as well as spin-orbit terms being omitted.) Many-body aspects of our findings unique to optimal incorporation of short- and long-range correlations within the CBF/FHNC formalism are analyzed. Where meaningful, our predictions for the density dependence of the gap at the Fermi wave number are compared with those from other microscopic calculations. Section 4 summarizes ways in which the present numerical study may be improved and extended.

2 Generic Many-Body Theory

2.1 The Normal Ground State

In this section, we briefly describe the Jastrow–Feenberg variational method and its implementation to superfluid systems. (For comprehensive background on this many-body approach and its generalization to the method of correlated basis functions, see Refs. [13, 15]. Recent descriptions and analysis of its applications to superfluid systems may be found in Refs. [18, 26].) We call this method “generic many-body theory” because the same equations can be derived by Green functions methods [27, 28], from coupled-cluster theory [29], and by a generalization of density functional theory to pair distribution functions [30], without mentioning a Jastrow–Feenberg wave function. We use the Jastrow–Feenberg point of view here because it is the simplest to implement and to generalize.

For a strongly interacting and translationally invariant *normal* system, the Jastrow–Feenberg theory assumes a non-relativistic many-body Hamiltonian

$$H = - \sum_i \frac{\hbar^2}{2m} \nabla_i^2 + \sum_{i < j} V(i, j). \tag{9}$$

The method starts with an *ansatz* for the wave function [31],

$$\Psi_0(\mathbf{r}_1, \dots, \mathbf{r}_N) = \frac{1}{\sqrt{I_{\mathbf{0},\mathbf{0}}}} F(\mathbf{r}_1, \dots, \mathbf{r}_N) \Phi_0(\mathbf{r}_1, \dots, \mathbf{r}_N), \tag{10}$$

$$F(\mathbf{r}_1, \dots, \mathbf{r}_N) = \exp \frac{1}{2} \left[\sum_{i < j} u_2(\mathbf{r}_i, \mathbf{r}_j) + \dots + \sum_{i_1 < \dots < i_n} u_n(\mathbf{r}_{i_1}, \dots, \mathbf{r}_{i_n}) + \dots \right], \tag{11}$$

where $I_{\mathbf{0},\mathbf{0}} = \langle \Phi_0 | F^\dagger F | \Phi_0 \rangle$ is a normalizing constant. Here $\Phi_0(\mathbf{r}_1, \dots, \mathbf{r}_N)$ denotes a model state, which for normal Fermi systems is a Slater-determinant, and F is a correlation operator written in general form, but to be truncated at the two-body u_2 term in a standard Jastrow calculation. There are basically two ways to deal with this type of wave function. In quantum Monte Carlo studies based on the fixed-node or constrained-path approximation, the trial wave function (10) is projected down to the true ground state by stochastic means, to the extent permitted by the Fermi sign problem, and an optimal correlation function $F(\mathbf{r}_1, \dots, \mathbf{r}_N)$ is obtained by stochastic means. Computationally far less demanding are diagrammatic methods, specifically the optimized Euler–Lagrange Fermi-hypernetted chain (FHNC-EL) method, which is well suited for calculation of physically interesting quantities. These diagrammatic methods have been successfully applied to such highly correlated Fermi systems as ^3He at $T = 0$ [32]. We have shown in recent work [33] that even the simplest version of the FHNC-EL theory is accurate within better than 1% at densities less than 25% of the saturation density of liquid ^3He , and the same or better performance is expected for nuclear systems.

The correlations $u_n(\mathbf{r}_1, \dots, \mathbf{r}_n)$ are obtained by minimizing the energy, i.e., by solving the Euler–Lagrange (EL) equations

$$E_0 = \langle \Psi_0 | H | \Psi_0 \rangle \equiv H_{\mathbf{0},\mathbf{0}}, \tag{12}$$

$$\frac{\delta E_0}{\delta u_n}(\mathbf{r}_1, \dots, \mathbf{r}_n) = 0. \tag{13}$$

Evaluation of the energy (12) for the variational wave function (10, 11) and analysis of the variational problem are carried out by cluster expansion and resummation methods. The procedure has been described at length in review articles [13,32] and pedagogical material [15]. Here, we spell out the simplest version of the equations that is consistent with the variational problem (“FHNC//0-EL”). These equations do not provide the quantitatively best implementation of this approach [32]. Instead, they provide the *minimal* version of the FHNC-EL theory. In particular, they contain the

indispensable physics, namely the correct description of both short- and long-ranged correlations.

In the FHNC//0-EL approximation, which contains both the random phase approximation (RPA) and the Bethe–Goldstone equation in a “collective” approximation, the Euler equation (13) can be written in the form

$$S(k) = \frac{S_F(k)}{\sqrt{1 + 2 \frac{S_F^2(k)}{t(k)} \tilde{V}_{p-h}(k)}}, \quad (14)$$

where $S(k)$ is the static structure factor of the interacting system, $t(k) = \hbar^2 k^2 / 2m$ is the kinetic energy of a free particle, $S_F(k)$ is the static structure factor of the non-interacting Fermi system, and

$$V_{p-h}(r) = [1 + \Gamma_{dd}(r)] V(r) + \frac{\hbar^2}{m} \left| \nabla \sqrt{1 + \Gamma_{dd}(r)} \right|^2 + \Gamma_{dd}(r) w_1(r) \quad (15)$$

is the so-called particle–hole interaction. As usual, we define the Fourier transform with a density factor, i.e.,

$$\tilde{f}(\mathbf{k}) \equiv \rho \int d^3r e^{i\mathbf{k}\cdot\mathbf{r}} f(\mathbf{r}). \quad (16)$$

Auxiliary quantities are the “induced interaction”

$$\tilde{w}_1(k) = -t(k) \left[\frac{1}{S_F(k)} - \frac{1}{S(k)} \right]^2 \left[\frac{S(k)}{S_F(k)} + \frac{1}{2} \right] \quad (17)$$

and the “direct–direct correlation function,”

$$\tilde{\Gamma}_{dd}(k) = (S(k) - S_F(k)) / S_F^2(k), \quad (18)$$

a “dressed” analog of the Fourier inverse of $\exp[u_2(r)] - 1$. Equations (14)–(18) form a closed set which can be solved by iteration. Note that the Jastrow correlation function $f(r) = \exp(u_2(r)/2)$ has been eliminated entirely.

More complicated versions of the FHNC-EL method add additional equations for the so-called ee, de, and cc diagrams which have been expressed in detail in Refs. [32, 34]; they will not be repeated here.

2.2 Correlated Basis Functions

Correlated basis functions (CBF) theory uses the correlation operator F to generate a complete set of basis states through

$$|\Psi_{\mathbf{m}}^{(N)}\rangle = \frac{F_N |\Phi_{\mathbf{m}}^{(N)}\rangle}{\langle \Phi_{\mathbf{m}}^{(N)} | F_N^\dagger F_N | \Phi_{\mathbf{m}}^{(N)} \rangle^{1/2}}, \quad (19)$$

where the $\{|\Phi_{\mathbf{m}}^{(N)}\rangle\}$ are Slater determinants of single-particle orbitals. We review the method only very briefly, the diagrammatic construction of the relevant ingredients having been derived in Ref. [35] (see also Ref. [32] for further details).

To develop a BCS theory with correlated wave functions, it is expedient to introduce a second-quantized formulation. The Jastrow–Feenberg correlation operator in (11) depends on the particle number, i.e., $F = F_N(1, \dots, N)$ (whenever unambiguous, we omit the corresponding subscript). Starting from the conventional a_k^\dagger, a_k operators that create and annihilate single-particle states, new creation and annihilation operators $\alpha_k^\dagger, \alpha_k$ of *correlated states* are defined by their action on the correlated basis states:

$$\alpha_k^\dagger |\Psi_{\mathbf{m}}\rangle \equiv \frac{F_{N+1} a_k^\dagger |\Phi_{\mathbf{m}}\rangle}{\langle \Phi_{\mathbf{m}} | a_k F_{N+1}^\dagger F_{N+1} a_k^\dagger | \Phi_{\mathbf{m}} \rangle^{1/2}}, \tag{20}$$

$$\alpha_k |\Psi_{\mathbf{m}}\rangle \equiv \frac{F_{N-1} a_k |\Phi_{\mathbf{m}}\rangle}{\langle \Phi_{\mathbf{m}} | a_k^\dagger F_{N-1}^\dagger F_{N-1} a_k | \Phi_{\mathbf{m}} \rangle^{1/2}}. \tag{21}$$

According to these definitions, α_k^\dagger and α_k obey the same commutation rules as the creation and annihilation operators a_k^\dagger and a_k of uncorrelated states, but they are not Hermitian conjugates of one another.

For off-diagonal elements $O_{\mathbf{m},\mathbf{n}}$ of an n -body operator O , we sort the quantum numbers m_i and n_i such that $|\Psi_{\mathbf{m}}\rangle$ is mapped onto $|\Psi_{\mathbf{n}}\rangle$ by

$$|\Psi_{\mathbf{m}}\rangle = \alpha_{m_1}^\dagger \alpha_{m_2}^\dagger \cdots \alpha_{n_d}^\dagger \alpha_{n_d} \cdots \alpha_{n_2} \alpha_{n_1} |\Psi_{\mathbf{n}}\rangle. \tag{22}$$

Then, the matrix elements $O_{\mathbf{m},\mathbf{n}}$ depend only on the *difference* between the states $|\Psi_{\mathbf{m}}\rangle$ and $|\Psi_{\mathbf{n}}\rangle$, and *not* on the states as a whole. Consequently, $O_{\mathbf{m},\mathbf{n}}$ can be written as the matrix element of a d -body operator

$$O_{\mathbf{m},\mathbf{n}} = \langle \Psi_{\mathbf{m}} | O | \Psi_{\mathbf{n}} \rangle \equiv \langle m_1 m_2 \dots m_d | \mathcal{O}(1, 2, \dots, d) | n_1 n_2 \dots n_d \rangle_a, \tag{23}$$

with the index a indicating antisymmetrization. In homogeneous systems, the continuous parts of the quantum numbers m_i, n_i are wave numbers $\mathbf{p}_i, \mathbf{p}'_i$; we abbreviate their difference as \mathbf{q}_i .

The key quantities for the execution of the theory are diagonal and off-diagonal matrix elements of unity and $H' \equiv H - H_{0,0}$,

$$M_{\mathbf{m},\mathbf{n}} = \langle \Psi_{\mathbf{m}} | \Psi_{\mathbf{n}} \rangle \equiv \delta_{\mathbf{m},\mathbf{n}} + N_{\mathbf{m},\mathbf{n}}, \tag{24}$$

$$H'_{\mathbf{m},\mathbf{n}} \equiv W_{\mathbf{m},\mathbf{n}} + \frac{1}{2} (H'_{\mathbf{m},\mathbf{m}} + H'_{\mathbf{n},\mathbf{n}}) N_{\mathbf{m},\mathbf{n}}. \tag{25}$$

Eq. (25) defines a natural decomposition [15,35] of the matrix elements of $H'_{\mathbf{m},\mathbf{n}}$ into the off-diagonal quantities $W_{\mathbf{m},\mathbf{n}}$ and $N_{\mathbf{m},\mathbf{n}}$ and diagonal quantities $H'_{\mathbf{m},\mathbf{m}}$. These diagonal matrix elements are additive to leading order in the particle number, allowing us to define the CBF single-particle energies e_m that satisfy

$$H'_{\mathbf{m},\mathbf{m}} = \langle \Psi_{\mathbf{m}} | H' | \Psi_{\mathbf{m}} \rangle \equiv \sum_{i=1}^d [e_{m_i} - e_{n_i}] + \mathcal{O}(N^{-1}). \tag{26}$$

According to Eq. (23), $W_{\mathbf{m},\mathbf{n}}$ and $N_{\mathbf{m},\mathbf{n}}$ define d -particle operators \mathcal{N} and \mathcal{W} , e.g.,

$$\begin{aligned} N_{\mathbf{m},\mathbf{o}} &\equiv N_{p_1 p_2 \dots p_d h_1 h_2 \dots h_d, 0} \\ &\equiv \langle p_1 p_2 \dots p_d | \mathcal{N}(1, 2, \dots, d) | h_1 h_2 \dots h_d \rangle_a, \\ W_{\mathbf{m},\mathbf{o}} &\equiv W_{p_1 p_2 \dots p_d h_1 h_2 \dots h_d, 0} \\ &\equiv \langle p_1 p_2 \dots p_d | \mathcal{W}(1, 2, \dots, d) | h_1 h_2 \dots h_d \rangle_a. \end{aligned} \tag{27}$$

Diagrammatic representations of $\mathcal{N}(1, 2, \dots, d)$ and $\mathcal{W}(1, 2, \dots, d)$ have the same topology [35]. In the next section, we will show that in dealing with pairing phenomena, only the two-body operators are needed.

In principle, $\mathcal{N}(1, 2)$ and $\mathcal{W}(1, 2)$ are non-local two-body operators. The leading, local contributions to these operators are readily expressed in terms of the diagrammatic quantities of FHNC-EL theory [32]:

$$\begin{aligned} \mathcal{N}(1, 2) &= \mathcal{N}(r_{12}) = \Gamma_{dd}(r_{12}), \\ \mathcal{W}(1, 2) &= \mathcal{W}(r_{12}), \quad \tilde{\mathcal{W}}(k) = -\frac{t(k)}{S_F(k)} \tilde{\Gamma}_{dd}(k). \end{aligned} \tag{28}$$

For further reference, we also display the coordinate space form of the interaction $\mathcal{W}(r_{12})$:

$$\begin{aligned} \mathcal{W}(r) &= V_{p-h}(r) + w_1(r), \\ &= [1 + \Gamma_{dd}(r)](v(r) + w_1(r)) + \frac{\hbar^2}{m} \left| \nabla \sqrt{1 + \Gamma_{dd}(r)} \right|^2, \end{aligned} \tag{29}$$

which exhibits somewhat more clearly the physical meaning of the individual terms: The factor $[1 + \Gamma_{dd}(r)]$ describes the short-ranged correlations, the term $(\hbar^2/m)|\nabla\sqrt{1 + \Gamma_{dd}(r)}|^2$ describes the cost in kinetic energy for bending the wave functions at short distances, and the induced potential $w_1(r)$ describes the corrections due to phonon exchange. In the local approximations spelled out in Eqs. (28), the CBF single-particle energies (26) assume the simple form

$$e_k = t(k) + \frac{\tilde{X}'_{cc}(k)}{1 - \tilde{X}_{cc}(k)} + \text{const.} \tag{30}$$

with

$$\tilde{X}'_{cc}(k) = -\frac{\rho}{v} \int d^3r e^{i\mathbf{k}\cdot\mathbf{r}} \mathcal{W}(r) \ell(rk_F), \tag{31}$$

$$\tilde{X}_{cc}(k) = -\frac{\rho}{v} \int d^3r e^{i\mathbf{k}\cdot\mathbf{r}} \Gamma_{dd}(r) \ell(rk_F), \tag{32}$$

where v ($= 2$) is the degree of degeneracy of the single-particle states, $\ell(x) = (3/x)j_1(x)$ is the Slater exchange function, and the constant is determined by the condition $e_{k_F} = \mu$. In the limit of a weakly interacting system, we have $\mathcal{W}(r) = v(r)$, and the e_k reduce to the Hartree–Fock single-particle energies (4).

2.3 BCS Theory with Correlated Wave Functions

The BCS theory of fermion superfluidity generalizes the Hartree–Fock model by introducing a superposition of independent-particle wave functions corresponding to different particle numbers [36], represented economically by Eq. (3) in terms of Bogoliubov amplitudes $u_{\mathbf{k}}, v_{\mathbf{k}}$.

The most natural way to deal with a strongly correlated system is to first project the bare-BCS state on an arbitrary member of a complete set of independent-particle states with fixed particle numbers. Then, apply the correlation operator to that state, normalize the result, and finally, sum over all particle numbers N . Thus, the correlated BCS (CBCS) state is taken as

$$|\text{CBCS}\rangle = \sum_{\mathbf{m}, N} |\Psi_{\mathbf{m}}^{(N)}\rangle \langle \Phi_{\mathbf{m}}^{(N)} | \text{BCS}\rangle. \tag{33}$$

The trial state (33) superposes the correlated basis states $|\Psi_{\mathbf{m}}^{(N)}\rangle$ with the same amplitudes the model states $|\Phi_{\mathbf{m}}^{(N)}\rangle$ have in the corresponding expansion of the *original* BCS vector. It is important to note that this state differs from the state proposed, analyzed, and applied computationally in Refs. [37–39], which fails to include the normalizing denominators present in Eq. (19). As shown in Ref. [17], this option leads to a meaningful gap equation only if specific diverging quantities are omitted.

Consider now the expectation value of an arbitrary two-body operator \hat{O} with respect to the superfluid state (33):

$$\langle \hat{O} \rangle_s = \frac{\langle \text{CBCS} | \hat{O} | \text{CBCS} \rangle}{\langle \text{CBCS} | \text{CBCS} \rangle}. \tag{34}$$

For superfluid gaps that are small compared to the Fermi energy, it suffices to consider the interaction of only one Cooper pair at a time. In that case, one need retain only the terms of *first order* in the deviation $v_{\mathbf{k}}^2 - v_{0,\mathbf{k}}^2$, where $v_{0,\mathbf{k}} = \theta(k_F - k)$ is the normal-state value, and those of *second order* in the product $u_{\mathbf{k}} v_{\mathbf{k}}$. We refer to this as the “decoupling approximation”. The error introduced thereby is of order $\varepsilon = (\Delta_F/e_F)^2$, where Δ_F is the superfluid gap energy at the Fermi energy e_F . Within this approximation, neither the pairing matrix elements nor the single-particle energies entering the gap equation depend on the Bogoliubov parameters $u_{\mathbf{k}}, v_{\mathbf{k}}$.

The calculation of $\langle \hat{H} - \mu \hat{N} \rangle_s$ for correlated states is somewhat tedious [16]. Details may be found in Refs. [16, 18]; we only give the final result. The energy of the superfluid state may be derived from

$$\begin{aligned} \langle \hat{H} - \mu \hat{N} \rangle_s &= H_{oo}^{(N)} - \mu N + 2 \sum_{\mathbf{k}, |\mathbf{k}| > k_F} v_{\mathbf{k}}^2 (e_{\mathbf{k}} - \mu) - 2 \sum_{\mathbf{k}, |\mathbf{k}| < k_F} u_{\mathbf{k}}^2 (e_{\mathbf{k}} - \mu) \\ &+ \sum_{\mathbf{k}, \mathbf{k}'} u_{\mathbf{k}} v_{\mathbf{k}} u_{\mathbf{k}'} v_{\mathbf{k}'} \mathcal{P}_{\mathbf{k}\mathbf{k}'} \end{aligned} \tag{35}$$

in terms of the “pairing interaction” specified by

$$\mathcal{P}_{\mathbf{k}\mathbf{k}'} = \mathcal{W}_{\mathbf{k}\mathbf{k}'} + (|e_{\mathbf{k}} - \mu| + |e_{\mathbf{k}'} - \mu|) \mathcal{N}_{\mathbf{k}\mathbf{k}'}, \tag{36}$$

$$\mathcal{W}_{\mathbf{k}\mathbf{k}'} = \langle \mathbf{k} \uparrow, -\mathbf{k} \downarrow | \mathcal{W}(1, 2) | \mathbf{k}' \uparrow, -\mathbf{k}' \downarrow \rangle_a, \tag{37}$$

$$\mathcal{N}_{\mathbf{k}\mathbf{k}'} = \langle \mathbf{k} \uparrow, -\mathbf{k} \downarrow | \mathcal{N}(1, 2) | \mathbf{k}' \uparrow, -\mathbf{k}' \downarrow \rangle_a. \tag{38}$$

With the result (35), we have arrived at a formulation of the theory which is isomorphic with the BCS theory for weakly interacting systems. Closer inspection [18] reveals that our approach corresponds to a BCS theory formulated in terms of the scattering matrix [40]. The correlation operator F serves here to tame the short-range dynamical correlations. The effective interaction $\mathcal{W}(1, 2)$ is just an energy-independent approximation of the T -matrix.

We may now implement the standard procedure of determining the Bogoliubov amplitudes $u_{\mathbf{k}}, v_{\mathbf{k}}$, by variation of the energy expectation (35). This leads to the familiar gap equation

$$\Delta_{\mathbf{k}} = -\frac{1}{2} \sum_{\mathbf{k}'} \mathcal{P}_{\mathbf{k}\mathbf{k}'} \frac{\Delta_{\mathbf{k}'}}{\sqrt{(e_{\mathbf{k}'} - \mu)^2 + \Delta_{\mathbf{k}'}^2}}. \tag{39}$$

The conventional (i.e., “uncorrelated” or “mean-field”) BCS gap equation [41] is retrieved by replacing the effective interaction $\mathcal{P}_{\mathbf{k}\mathbf{k}'}$ by the pairing matrix of the bare interaction. The low-cluster-order approximations to the pairing interaction used by Benhar [42] and Pavlou et. al. [22] are obtained by setting $\Gamma_{dd}(r) \approx f^2(r) - 1$ in Eqs. (28) and (29) and omitting the induced interaction $w_I(r)$.

3 Application to Neutron Matter

3.1 Energetics

We have carried out ground-state calculations for static properties and superfluid pairing gaps in neutron matter based on two representative NN interactions acting in the $T = 1$ channel, namely the central parts of the Reid soft-core potential [7] as formulated in Eqs. (A.1)–(A.8) of Ref. [43], generally referred to as Reid V_6 , and the Argonne V'_4 potential [23]. In the density regime where the 1S_0 pairing gap has significant amplitude, any interaction must give very close to the same E/N for nuclear matter

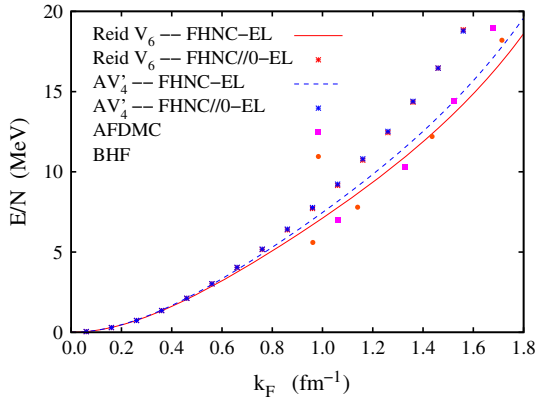


Fig. 1 Neutron-matter equation of state for the central component of the Reid V_6 soft-core potential (red line and asterisks) and for the Argonne V'_4 potential (blue dashed line and asterisks), as obtained by a full FHNC-EL calculation (solid lines) and from the simple FHNC//0-EL approximation (asterisks). Included for comparison are results from the auxiliary-field diffusion Monte Carlo (AFDMC) method [44] for the Argonne V_{18} interaction (magenta squares) and from a Brueckner–Hartree–Fock (BHF) calculation [45] for the Argonne V'_4 potential (orange dots) (Color figure online)

and the deuteron, as long as it fits the S -wave scattering data and the deuteron. We have carried out two types of calculations: Full FHNC-EL calculations as described, for example, in Refs. [32, 34], and FHNC//0-EL calculations as described in Sect. 2.1. Results for the equation of state for these two calculations, plotted as E/N versus Fermi momentum k_F , are shown in Fig. 1.

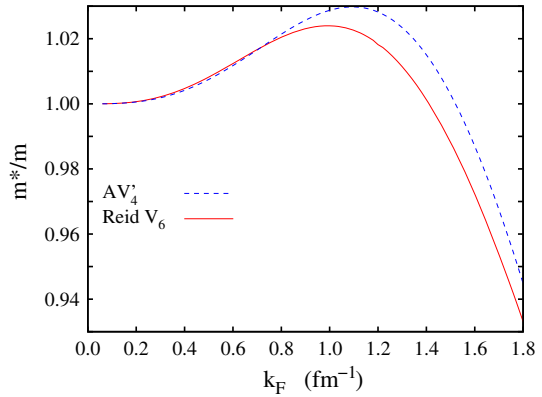
The picture is very similar to that found for Lennard–Jones interactions [33]: The FHNC//0 approximation performs well up to about half nuclear saturation density. It is also noteworthy that the two potentials lead to very nearly the same equation of state in the density range considered, with the asterisks for the respective FHNC//0-EL calculations overlapping.

For the Reid potential, we have also examined the importance of optimized triplet correlations, i.e., non-vanishing u_3 in Eq. (11) and elementary-diagram cluster contributions as outlined in Ref. [32] and found their influence negligible. We have also tried the central part of the full Argonne V_{18} potential in the $T = 1$ channel. It turns out that this component of the interaction is too soft to lead to a stable solution of the Euler equation. The problem can be solved by an artificial enhancement of the repulsive regime, but the results depend sensitively on that enhancement factor and hence were considered unreliable.

3.2 BCS Pairing

Once the ground-state correlations are known, the superfluid gap function $\Delta_{\mathbf{k}}$ can be determined by solving the gap equation (39). Since we are concerned with 1S_0 pairing, we have inserted the 1S_0 component of the chosen potential model into the effective interaction (29). In the phonon-exchange correction $w_1(r)$, the central component of the interaction is the appropriate choice.

Fig. 2 Neutron effective mass for the central component of the Reid V_6 soft-core potential (solid red line) and for the Argonne V'_4 potential (dashed blue line), as derived from the CBF single-particle spectrum (30). Recall that the gap increases monotonically with the effective mass, see Fig. 3 (Color figure online)



The gap equation was solved by the eigenvalue method with an adaptive mesh, as outlined in appendix of Ref. [18]. We have primarily adopted a free single-particle spectrum for $e_{\mathbf{k}}$ as it occurs in Eqs. (36) and (39). One could also use the actual spectrum of CBF single-particle energies (30), calculated from the effective interactions [35], in both the pairing interaction (36) and the denominator of Eq. (39). We have not done this for the reason outlined below.

At first glance, only the spectrum in the vicinity of the Fermi momentum is relevant. In that regime, it can be approximated quite well in terms of an effective mass. Figure 2 shows the effective mass obtained from the CBF single-particle energies for both potential models.

Evidently, the effective-mass ratio m^*/m obtained for both potentials is very close to unity.

However, “first glance” may not be sufficient; there is a subtlety to consider: If the gap at the Fermi surface is small, we can replace the pairing interaction $\tilde{\mathcal{W}}(k)$ by its S -wave matrix element at the Fermi surface,

$$\tilde{\mathcal{W}}_F \equiv \frac{1}{2k_F^2} \int_0^{2k_F} k dk \tilde{\mathcal{W}}(k) = N \mathcal{W}_{k_F, k_F}. \tag{40}$$

Then, we can write the gap equation as

$$1 = -\tilde{\mathcal{W}}_F \int \frac{d^3k'}{(2\pi)^3 \rho} \left[\frac{1}{\sqrt{(e_{k'} - \mu)^2 + \Delta_{k_F}^2}} - \frac{|e_{k'} - \mu|}{\sqrt{(e_{k'} - \mu)^2 + \Delta_{k_F}^2}} \frac{S_F(k')}{t(k')} \right], \tag{41}$$

which is almost identical to Eq. (16.91) in Ref. [40]. In particular, the second term, which originates from the energy numerator generated in Eq. (39) by the second term of $\mathcal{P}_{\mathbf{k}\mathbf{k}'}$ in Eq. (36), has the function of regularizing the integral for large k' . This feature is lost if the bare mass is used in the relationship (28), and the integral (41) diverges unless a momentum-dependent effective mass ratio is used that approaches unity in the limit of large momenta.

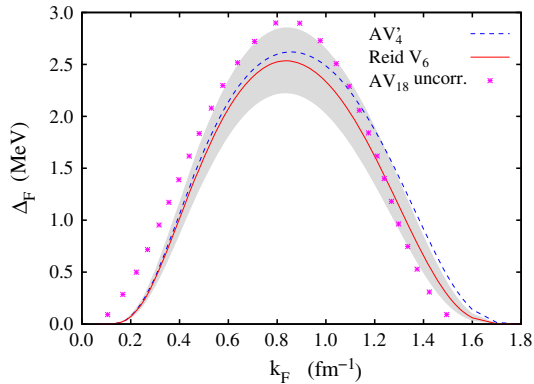


Fig. 3 Superfluid gap Δ_{k_F} at the Fermi momentum as a function of Fermi wave number k_F for the Reid V_6 soft-core interaction (solid red curve) and the Argonne V_4' potential (dashed blue curve). The gray shaded area shows the range of influence an effective-mass correction can have: The lower boundary of that area corresponds to $m^*/m = 0.95$ and the upper boundary to $m^*/m = 1.05$. Included for comparison are results from a pure (“uncorrelated”) BCS gap calculation for the Argonne V_{18} interaction (red asterisks) (Color figure online)

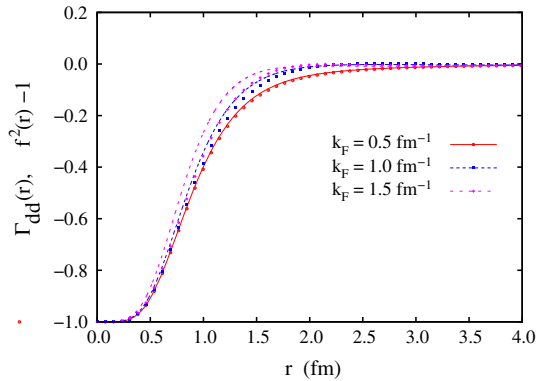
A second issue is that it has been known for a long time [46,47] that the effective mass in nuclear systems has a peak around the Fermi surface; however, such a peak is absent in the CBF single-particle spectrum. An effective-mass enhancement may be obtained by including complex self-energy corrections; this can be done, for example, by going to higher-order terms in CBF perturbation theory [48]. We note that the enhancement effect is much stronger in ^3He (see Refs. [49–51]) due to the softness of the spin-fluctuation mode.

In view of these considerations, we have deemed it more accurate to employ the free single-particle spectrum $e_k = t(k)$, and to study the *sensitivity* of our results to changes in the effective mass. Our results for the superfluid gap for the two potential models are shown in Fig. 3. Evidently, the difference of the gap between these two potential models is almost negligible and certainly within the accuracy of the FHNC approximations. To determine the importance of effective-mass corrections, we have also solved the gap equation assuming effective-mass ratios between $m^*/m = 0.95$ and $m^*/m = 1.05$ in both the pairing interaction (36) and the energy denominator (2). The results for the gap define the gray area in Fig. 3; their spread provides a conservative estimate of the importance of a non-trivial single-particle spectrum.

3.3 Consequences for Many-Body Theory

To conclude this section, let us look more closely at different aspects of the convergence of cluster expansion and resummation techniques. Apart from cold atomic gases—which with rare exceptions like the “unitary limit” pose no challenges to modern many-body theory—pure neutron matter at subnuclear and nuclear densities is, apart from the complications introduced by the NN force, one of the most lenient many-particle systems provided by nature. This is largely due to the low density of the system, as measured for example by the ratio of the pion Compton wavelength [7],

Fig. 4 Plots of the “dressed” correlation function $\Gamma_{dd}(r)$ (solid lines) for three representative densities, as indicated in the legend. Also shown is the pair correlation function $f^2(r) - 1$ (dotted lines). Note that this function is calculated a posteriori from the solution of the Euler equation; the generic many-body method spelled out in Sect. 2.1 never needs to introduce this quantity (Color figure online)



$\lambda_\pi = 1/\mu_\pi = \hbar/m_\pi c \approx 1.4$ fm, or the radius of the “hard core,” $\sigma \sim 0.7 - 0.9$ fm, to the average particle spacing at the given density $\rho = k_F^3/3\pi^2$. Thus, at $k_F = 1.4$ fm⁻¹ the density is $\rho \approx 0.06\sigma^{-3}$, which corresponds to only 20% of the saturation density of ³He.

Evidence for the good convergence of many-body theory for neutron matter in the density regime relevant for ¹S₀ pairing is already provided in Fig. 1, which shows that the very simple FHNC//0 approximation for the energy is quite accurate. In fact, even the very simple two-body cluster approximation

$$\left(\frac{E}{N}\right)_2 = \frac{T_F}{N} + \frac{\rho}{2} \int d^3r \left[(1 + \Gamma_{dd}(r)) v(r) + \frac{\hbar^2}{m} \left| \nabla \sqrt{1 + \Gamma_{dd}(r)} \right|^2 \right] g_F(r), \tag{42}$$

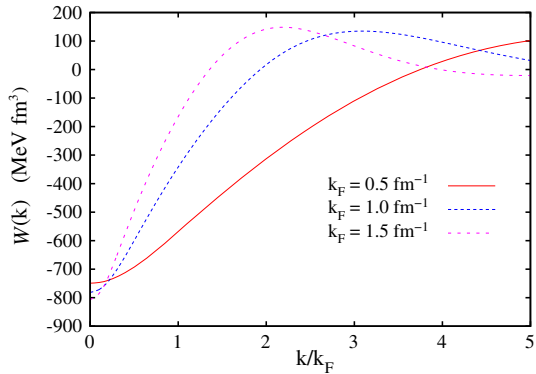
in which T_F is the kinetic energy of the free Fermi gas and $g_F(r) = 1 - \ell^2(rk_F)/2$ its pair distribution function, yields results virtually identical to the FHNC//0 results plotted in Fig. 1. We have refrained from showing these results in order not to obscure the figure. Note that one can of course identify $1 + \Gamma_{dd}(r)$ with $f^2(r)$ in Eq. (42).

These findings are consistent with the fact that the optimal results for $1 + \Gamma_{dd}(r)$ and $f^2(r)$ are not very different. To demonstrate this, both functions are plotted in Fig. 4 for three representative densities, i.e., $k_F = 0.5, 1.0,$ and 1.5 fm⁻¹. At the lowest density, the two functions are practically identical. As the density increases, $\Gamma_{dd}(r)$ becomes slightly steeper in the attractive regime of the interaction.

From these results, one might be led to conclude that low-order methods are also adequate for calculating the superfluid gap. We remind the reader, however, of the discussions in Sect. 1.3 on the both the sensitivity of quantities other than the energy to the correlation functions, and to the convergence rate of cluster expansions. Accordingly, we have examined the consequences of two approximations: leaving out the energy numerator generated by the pairing interaction (36) and leaving out the induced interaction $w_I(r)$.

The most important function of the energy numerator is to regularize the integral in the gap equation for contact interactions, as witnessed in Eq. (41). The situation being discussed at that point is, of course, extreme. More generally, one would expect

Fig. 5 Momentum dependence of the pairing interaction $\mathcal{W}(k) \equiv \tilde{\mathcal{W}}(k)/\rho$ for three representative densities as indicated in the legend (Color figure online)



that the energy-numerator term is important whenever the pairing interaction $\tilde{\mathcal{W}}(k)$ does not fall off sufficiently rapidly for large momenta. This is indeed the case: We show in Fig. 5 the interaction $\tilde{\mathcal{W}}(k)$ for three representative densities. Evidently, the pairing interaction does not fall off rapidly above k_F . The effect is, of course, most pronounced for low densities. Although the gap is determined solely by the pairing matrix element $\tilde{\mathcal{W}}_F$ in the limit of an infinitesimal gap, one must expect significant finite-range effects in the present case where the gap is of the order of 10–50% of the Fermi energy.

The second new aspect is the appearance of the induced interaction term $w_1(r)$ appearing in the pairing interaction [cf. Eqs. (29) and (17)]. This term describes the exchange of particle–hole excitations [27] and is one of the important effects introduced into the CBF version of BCS theory. While the gap equation includes the summation of ladder diagrams [4,52] and can, at least in principle, deal with bare hard-core interactions, the particle–hole reducible diagrams described by $w_1(r)$ introduce new physics.

Ignoring the induced interaction $w_1(r)$ leads to the two-body approximation

$$\mathcal{W}_2(r) = [1 + \Gamma_{dd}(r)] v(r) + \frac{\hbar^2}{m} \left| \nabla \sqrt{1 + \Gamma_{dd}(r)} \right|^2 \tag{43}$$

for the pairing interaction. We note that in this case one can again identify $\Gamma_{dd}(r) \Rightarrow f^2(r) - 1$.

Figure 6 demonstrates the impact on the calculated energy gap of the two approximations identified above, for the case of the Reid potential. Evidently, both simplifications have rather dramatic effects, being enhanced by the nominally exponential dependence of the gap on the pairing interaction. At this point, we are not prepared to describe or affirm any systematics of the effects of these approximations. However, the close proximity of the “full CBCS” results and those for the bare interaction shown in Fig. 3 would seem to be coincidental, stemming from competing corrections.

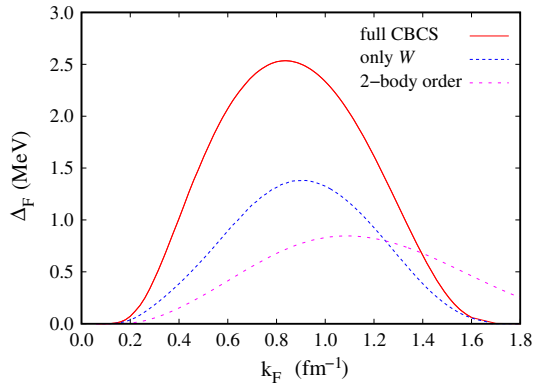


Fig. 6 This figure shows the consequences of the two approximations discussed in the text for the magnitude of the gap at the Fermi surface. The curve “full CBCS” (red) is identical to that shown in Fig. 3; the curve “only W ” (blue) shows the consequence of omitting the energy-numerator term generated by the CBF pairing interaction, and the curve “two-body order” (magenta) is obtained by using the two-body approximation (43) while also leaving out the energy-numerator term. In this last case, inclusion of the energy-numerator term does not lead to sensible results because the cancellation illustrated by Eq. (41) is violated (Color figure online)

3.4 Comparison with Previous Gap Calculations

The work we report represents the most rigorous calculation yet performed for nuclear systems within correlated BCS theory. It is therefore of special interest to compare its results with those of earlier calculations of the 1S_0 pairing gap for neutron matter based on microscopic many-body theories, where meaningful conclusions might be drawn.

Informative comparison of the predictions of previous gap calculations—as represented for example by the aforementioned summary figure in the review by Gezerlis et al. [24]—is rendered problematic by the diversity of methods applied, interactions adopted, and assumptions made (e.g., whether or not polarization effects from exchange of density and/or spin-density fluctuations are included). Nevertheless, some specific and non-specific comparisons may be useful.

Figure 3 includes data plotted for a pure-BCS calculation in which the pairing interaction is the bare potential in the 1S_0 channel of the Argonne V_{18} interaction, used along with free single-particle e_k . The BCS result for Argonne V_{18} , calculated by the separation method of Ref. [9], was taken from Ref. [53]. (For this present purpose, the distinction between the original Argonne V_{18} interaction and Argonne V'_4 should be immaterial.) Corresponding bare-BCS results for the Reid V_6 choice (displayed in Ref. [9] but not plotted here) are very close to those shown for Argonne V_{18} , as expected. What is unexpected is that our CBF results for the Argonne case show only a modest suppression (about 15%) of the Δ_F maximum, which occurs slightly above 0.8 fm^{-1} in both calculations. The approximately Gaussian shape of Δ_F versus k_F shifts to slightly lower k_F in the absence of Jastrow–Feenberg correlations. It is obvious from Fig. 6 that this near concurrence cannot be attributed to unimportance of the correlations introduced in the CBF treatment. It is possible that this feature is due

in part to the presence of the induced interaction term $w_1(r)$ in the effective pairing interaction coming from density fluctuations, which is expected to enhance the gap relative to that given by direct part of $\mathcal{W}(r)$.

The most recent microscopic calculations of the 1S_0 gap incorporating Jastrow–Feenberg two-body correlations are those of Pavlou et al. [22], described briefly in Sect. 1.3. Their variational CBF study was carried out for each of two different parametrized forms of the Jastrow factor $f(r)$, subject to a constraint on its “wound,” as outlined briefly in Sect. 1.3. Both of these forms have been used in earlier work: one, referred to as the “Benhar” choice, has one free parameter but allows $f(r)$ to overshoot unity, whereas the “Davé” choice has two free parameters but no overshoot. Restricted minimization was performed on an approximation to the energy expectation E/N that retains only the leading (zeroth) order of its cluster expansion, neglecting terms of first and higher orders in a dimensionless small parameter ξ that grows with density. (While its value remains well below 0.05 in the relevant density regime, the implied rate of convergence of the expansion of E/N does not extend to approximants of Δ_F .)

The approach adopted in Ref. [22] may be considered the simplest implementation of correlated CBF theory. The effective pairing interaction it generates differs from its FHNC-EL counterparts in two essential respects: It lacks precisely those ingredients that are the subjects of the above discussion of the “many-body consequences” of our work based on FHNC-EL theory, namely the energy-numerator term and the induced interaction entering the effective interaction \mathcal{W} .

This same statement applies to the variational component of the correlated BCS approach applied much earlier by Chen et al. [8], in which the 1S_0 gap in neutron matter was estimated based on the central, V_4 part of the Reid V_6 soft-core interaction. In that case, Δ_F was found to peak at about 0.75 fm^{-1} with a maximum value close to 3.2 MeV , a result based in fact on the Davé form for $f(r)$. It should then be no surprise that with negligible differences, Pavlou et al. obtained almost exactly the same result for Δ_F versus k_F , although the Argonne V_{18} interaction was assumed. It should be said that all of the tests we have made support the assertion that, when the 1S_0 gap is calculated by the same method with different inputs for the bare NN interactions but otherwise the same assumptions (e.g., for the single-particle energies e_k), virtually identical results will be obtained for Δ_F , provided the NN interaction chosen reproduces the NN scattering data up to laboratory energies relevant for k_F below about 1.5 fm^{-1} . Indeed, this a well-established property for the BCS gap [54].

As already pointed out, the maximum gap value obtained by Pavlou et al. with AV_{18} for their two optimized correlation functions differ by nearly a factor two (about 3.7 MeV for the Davé form at $k_F = 0.85 \text{ fm}^{-1}$ and 1.8 MeV at $k_F = 0.75 \text{ fm}^{-1}$ for the Benhar choice)—reflecting the extreme sensitivity of the gap to inputs for the effective interaction. Recognizing that the induced interaction and energy-numerator terms are absent in these two calculations, the information provided by Fig. 6 on the relative contributions of these additional terms suggests that the results obtained in Ref. [22] for the Benhar correlation function are to be favored over those for the Davé form.

Turning to other microscopic calculations designed to provide accurate predictions for the 1S_0 gap in neutron matter, we first single out the study of Cao, Lombardo, and Schuck [55], carried out within the framework of Brueckner theory. Mean-field theory

for the superfluid state, as represented by the pure-BCS treatment, was modified by replacement of the bare pairing interaction with a proper vertex part, which includes an induced interaction describing the competition between the attractive density excitations and their repulsive spin-density counterparts (i.e., screening or polarization corrections [56]). In-medium corrections were also introduced into the self-energies e_k , corresponding to both dispersion and Fermi-surface depletion. The quenching of the gap due to exchange of spin-density fluctuations was found to be less extreme than indicated by some previous studies. Results based on a free single-particle spectrum were also reported, allowing more direct comparison with our results. For the free spectrum, Cao et al. [55] find a maximum Δ_F of about 2.7 MeV occurring close to $k_F = 0.85 \text{ fm}^{-1}$, based on the Argonne V_{18} interaction. The close agreement with our CBCS results shown in Fig. 3 is remarkable, but provocative, as our treatment does not include an induced interaction term corresponding to spin-density fluctuations. On the other hand, the treatment of screening effects in the two approaches is not directly comparable. For a recent intensive computational analysis of medium polarization in asymmetric nuclear matter, see Refs. [56,57].

The auxiliary-field diffusion Monte Carlo algorithm (AFDMC) purports to yield accurate results for pairing gaps in neutron matter and other many-fermion systems [44,58]. This algorithm has two essential features, not unique to AFDMC:

- (i) Unlike the BCS state, the trial wave function Ψ_T that is propagated in imaginary time describes a definite number of particles N , even or odd. The part of Ψ_T that describes pairing is essentially the projection of the BCS state onto the N -particle Hilbert space, which is a Pfaffian. Correlations are otherwise introduced into Ψ_T by a Jastrow factor.
- (ii) The pairing gap is constructed as a difference of energies obtained for different particle numbers,

$$\Delta = E(N) - \frac{1}{2} [E(N+1) + E(N-1)]. \quad (44)$$

Whatever the merits and deficits of the AFDMC approach, which implements a uniquely economical strategy in sampling the spin degrees of freedom, they differ significantly from those of traditional, analytically oriented many-body theory. Consequently, AFDMC tends to be regarded as one potentially independent arbiter in judging the quality of such traditional methods when valid comparisons can be made. The number of data points shown in Ref. [58] for the 1S_0 gap in neutron matter does not allow a reliable identification of the peak value of Δ_F , but it would lie slightly above 2 MeV, reached slightly above $k_F = 0.6 \text{ fm}^{-1}$. This calculation is based on a bare pairing interaction of V_6 form, obtained by deleting the two spin-orbit components of the Argonne V'_8 potential.

A more established alternative for arbitration is the Green Function Monte Carlo (GFMC) method, which has been applied to neutron matter by Gerzelis and Carlson [59,60]. Five data points are reported for Δ_F versus k_F (as shown in Fig. 6 of Pavlou et al.). These data extend only to a k_F value slightly beyond 0.5 fm^{-1} , where the gap is about 1 MeV (with an error bar of about 0.2), well below the interpolated result of Gandolfi et al. [58] at this density. It appears unlikely that, if the calculation were

extended, the GFMC gap value would reach 1.5 MeV. The bare interaction, which includes only S - and P -wave parts, is assumed and hence is essentially equivalent to Argonne V_4 .

This comparison of different Monte Carlo results is another testament to the sensitivity of the pairing gap calculations to the microscopic input, whether this input is the interaction itself, methodological assumptions within a traditional many-body theory, or the trial function Ψ_T for initiating Monte Carlo simulation. We discuss the two Monte Carlo studies to provide a more balanced perspective on the current status of the problem, but restrain from drawing conclusions about their relative merit or their bearing on the quality of our calculations.

4 Summary and Prospects

In this paper, we have described new calculations of the pairing gap in the 1S_0 partial-wave channel. Our findings have been analyzed and discussed in the preceding section.

The most interesting result of previous [18] work along these lines is the appearance of a divergence of solutions of the FHNC-EL equations that occurs, as a function of potential strength, well before the divergence of the vacuum scattering length a_0 of the interaction potential. This divergence of solutions of the FHNC-EL equations is analogous to the spinodal instability often discussed in earlier literature, with the principled and practical conclusion that the FHNC-EL equations for the *homogeneous* system have no solutions if $F_0^s < -1$, i.e., if the system is unstable in the particle–hole channel. In Ref. [18], divergence of the FHNC-EL equations in the case of a diverging in-medium scattering length gave evidence that the ground state is unstable against dimerization. The appearance of such instabilities whenever the assumptions on the state of the system fail—here, assumption of a non-dimerized phase, in the case of particle–hole instabilities, of a uniform system—is a unique feature of theories such as FHNC-EL that enjoy the topological completeness of parquet diagrams.

In the calculations being reported, we have not encountered such an instability, which could be taken as evidence that medium-driven formation of dineutrons in low-density neutron matter does not occur, or, in current terminology, that a BEC–BCS crossover [61–64] does not take place. This is remarkable in view of the fact that, at low densities ($k_F \approx 0.2 \text{ fm}^{-1}$), the gap reaches 0.45 times the Fermi energy e_F which is not much less than what is found in the unitary Fermi gas at the BCS–BEC crossover [65]; see also Ref. [60] who pointed this out more recently. It should also be mentioned that a recent study [66] of the phase diagram of spin-polarized neutron matter revealed signatures that can be interpreted [52] as a precursor of such a crossover.

There are four areas where the present calculation can be improved:

- (a) As pointed out above, the FHNC-EL method sums all ring and ladder diagrams. It does that, however, in a “collective approximation” of the particle–hole and the particle–particle propagators [32] that treats the correlations between particles within the Fermi sea in an average way. Since pairing occurs between particles at the Fermi surface, it must be examined to what extent the average treatment of correlations is appropriate. The route to improve upon this aspect is well

charted within CBF theory, and earlier studies [67,68] have demonstrated that CBF corrections to the pairing matrix elements can indeed be significant.

- (b) Related to (a): Whereas the effect of density fluctuations (exchange of virtual phonons) has been included in the CBF pairing interaction in an average-propagator sense, effects of spin-density fluctuations are not taken into account. Based on Landau parameters and some microscopic efforts [8,69–71], density fluctuations produce a modest enhancement of the pairing gap, whereas the spin-density channel generates a dominant suppression. Without introducing explicit spin-dependent correlations into the basis functions of the CBF treatment, their perturbative treatment within the CBF framework would be required.
- (c) In the present work, in-medium effects on the self-energy input e_k to the gap equation have not been pursued quantitatively. This shortcoming warrants further attention in subsequent applications of correlated BCS theory.
- (d) The most severe approximation made in this work is the use of state-independent correlation functions, albeit the two-nucleon interaction is exquisitely state dependent. Introduction of a correlation operator F in Eq. (10) that contains spin-, isospin-, tensor-, and more complicated operators in the two-body correlation vehicle $u_2(ij)$ figuratively opens Pandora’s box. This complexity has been largely dealt with in rather simple approximations that either completely omit commutator terms [72,73] or in a “single-operator-chain” approximation [74], which only sums the ring diagrams of state-dependent correlations. Unfortunately, for modern nucleon–nucleon interactions, which may have different core sizes in the singlet and triplet channels, the contributions of commutator diagrams can be huge [75]. It remains to be seen how important these effects are in the problem considered here, but at higher densities they can be decisive.

Acknowledgements This work was supported, in part, by the College of Arts and Sciences, University at Buffalo SUNY, and the Austrian Science Fund Project I602 (to EK). JWC acknowledges support from the McDonnell Center for the Space Sciences and expresses gratitude to the University of Madeira and its branch of Centro de Investigação em Matemática e Aplicações (CIMA) for gracious hospitality during periods of extended residence.

References

1. J. Bardeen, L.N. Cooper, J.R. Schrieffer, *Phys. Rev.* **108**, 1175 (1957)
2. R. Broglia, V. Zelevensky, *Fifty Years of Nuclear BCS* (World Scientific, Singapore, 2013)
3. A. Bohr, B.R. Mottelson, D. Pines, *Phys. Rev.* **110**, 936 (1958)
4. L.N. Cooper, R.L. Mills, A.M. Sessler, *Phys. Rev.* **114**, 1377 (1959)
5. J.R. Schrieffer, *Theory Of Superconductivity (Advanced Books Classics)*, revised edn. (Perseus Books, New York, 1999)
6. R.L. Mills, A.M. Sessler, S.A. Moszkowski, D.G. Shankland, *Phys. Rev. Lett.* **3**, 381 (1959)
7. R.V. Reid Jr., *Ann. Phys. (NY)* **50**, 411 (1968)
8. J.M.C. Chen, J.W. Clark, R.D. Davé, V.V. Khodel, *Nucl. Phys. A* **555**, 59 (1993)
9. V.A. Khodel, V.V. Khodel, J.W. Clark, *Nucl. Phys. A* **598**, 390 (1996)
10. J.W. Clark, C.H. Yang, *Lett. Nuovo Cimento* **3**, 272 (1970)
11. C.H. Yang, J.W. Clark, *Nucl. Phys. A* **174**, 49 (1971)
12. C.H. Yang, Ph.D. thesis, Washington University, 1971

13. J.W. Clark, in *Progress in Particle and Nuclear Physics*, vol. 2, ed. by D.H. Wilkinson (Pergamon Press Ltd., Oxford, 1979), pp. 89–199
14. N.C. Chao, J.W. Clark, C.H. Yang, Nucl. Phys. A **179**, 320 (1972)
15. E. Krotscheck, in *Introduction to Modern Methods of Quantum Many-Body Theory and their Applications, Advances in Quantum Many-Body Theory*, vol. 7, ed. by A. Fabrocini, S. Fantoni, E. Krotscheck (World Scientific, Singapore, 2002), pp. 267–330
16. E. Krotscheck, R.A. Smith, A.D. Jackson, Phys. Rev. B **24**, 6404 (1981)
17. E. Krotscheck, J.W. Clark, Nucl. Phys. A **333**, 77 (1980)
18. H.H. Fan, E. Krotscheck, T. Lichtenegger, D. Mateo, R.E. Zillich, Phys. Rev. A **92**, 023640 (2015)
19. J.W. Clark, A. Sedrakian, M. Stein, X.G. Huang, V.A. Khodel, V.R. Shaginyan, M.V. Zverev, J. Phys. Conf. Ser. **702**, 012012 (2016)
20. L. Gorkov, T.K. Melik-Barkhudarov, Sov. Phys. JETP **13**, 1018 (1961)
21. H. Heiselberg, C.J. Pethick, H. Smith, L. Viverit, Phys. Rev. Lett. **85**, 2418 (2000)
22. G.E. Pavlou, E. Mavrommatis, C. Moustakidis, J.W. Clark, Eur. Phys. J. A **53**, 96 (2017)
23. R.B. Wiringa, V.G.J. Stoks, R. Schiavilla, Phys. Rev. C **51**, 38 (1995)
24. A. Gezerlis, C.J. Pethick, A. Schwenk, in *Novel Superfluids*, vol. 2, ed. by K.H. Bennemann, J.B. Ketterson (Oxford University Press, Oxford, 2014). Chap. 22
25. R.B. Wiringa, S.C. Pieper, Phys. Rev. Lett. **89**, 182501 (2002)
26. J.W. Clark, in *Fifty Years of Nuclear BCS*, ed. by R.A. Broglia, V. Zelevinsky (World Scientific, Singapore, 2013), pp. 360–376. Chap. 27
27. A.D. Jackson, A. Lande, R.A. Smith, Phys. Rep. **86**(2), 55 (1982)
28. A.D. Jackson, A. Lande, R.A. Smith, Phys. Rev. Lett. **54**, 1469 (1985)
29. R.F. Bishop, in *Condensed Matter Theories*, vol. 10, ed. by M. Casas, J. Navarro, A. Polls (Nova Science Publishers, Commack, New York, 1995), pp. 483–508
30. E. Krotscheck, Phys. Lett. A **190**, 201 (1994)
31. E. Feenberg, *Theory of Quantum Fluids* (Academic, New York, 1969)
32. E. Krotscheck, J. Low Temp. Phys. **119**, 103 (2000)
33. J. Egger, E. Krotscheck, R.E. Zillich, J. Low Temp. Phys. **165**, 275 (2011)
34. E. Krotscheck, Ann. Phys. (NY) **155**, 1 (1984)
35. E. Krotscheck, J.W. Clark, Nucl. Phys. A **328**, 73 (1979)
36. S.T. Beliaev, in *Lecture Notes of the 1957 Les Houches Summer School*, ed. by C. DeWitt, P. Nozières (Dunod, Paris, 1959), pp. 343–374
37. S. Fantoni, Nucl. Phys. A **363**, 381 (1981)
38. A. Fabrocini, S. Fantoni, A.Y. Illarionov, K.E. Schmidt, Phys. Rev. Lett. **95**, 192501 (2005)
39. A. Fabrocini, S. Fantoni, A.Y. Illarionov, K.E. Schmidt, Nucl. Phys. A **803**, 137 (2008)
40. C.J. Pethick, H. Smith, *Bose–Einstein Condensation in Dilute Gases*, 2nd edn. (Cambridge University Press, Cambridge, 2008)
41. A.L. Fetter, J.D. Walecka, *Quantum Theory of Many-Particle Systems* (McGraw-Hill, New York, 1971)
42. O. Benhar, G.D. Rosi, G. Salvi, J. Low Temp. Phys. (2017). (This volume, [arXiv:1305.4659](https://arxiv.org/abs/1305.4659))
43. B.D. Day, Phys. Rev. C **24**, 1203 (1981)
44. S. Gandolfi, A. Illarionov, K.E. Schmidt, F. Pederiva, S. Fantoni, Phys. Rev. C **79**, 054005 (2009)
45. M. Baldo, A. Polls, A. Rios, H.J. Schulze, I. Vidaña, Phys. Rev. C **86**, 064001 (2012)
46. G. Brown, J. Gunn, P. Gould, Nucl. Phys. **46**, 598 (1963)
47. P. Quentin, H. Flocard, Ann. Rev. Nucl. Part. Sci. **28**, 523 (1978)
48. E. Krotscheck, R.A. Smith, A.D. Jackson, Phys. Lett. B **104**, 421 (1981)
49. G.E. Brown, C.J. Pethick, A. Zaringhalam, J. Low Temp. Phys. **48**, 349 (1982)
50. B.L. Friman, E. Krotscheck, Phys. Rev. Lett. **49**, 1705 (1982)
51. E. Krotscheck, J. Springer, J. Low Temp. Phys. **132**(5/6), 281 (2003)
52. P. Nozières, S. Schmitt-Rink, J. Low Temp. Phys. **59**, 195 (1985)
53. L. Yuan, Three-body pairing interaction effect on superfluidity with applications to neutron star matter. Ph.D. thesis Washington University, 2011
54. Ø. Elgarøy, M. Hjorth-Jensen, Phys. Rev. C **57**, 1174 (1998)
55. L.G. Cao, U. Lombardo, P. Schuck, Phys. Rev. C **74**, 064301 (2006)
56. H.J. Schulze, A. Polls, A. Ramos, Phys. Rev. C **63**, 044310 (2001)
57. S.S. Zhang, L.G. Cao, U. Lombardo, P. Schuck, Phys. Rev. C **93**, 044329 (2016)
58. S. Gandolfi, A. Illarionov, F. Pederiva, K.E. Schmidt, S. Fantoni, Phys. Rev. C **80**, 045802 (2009)
59. A. Gezerlis, J. Carlson, Phys. Rev. C **77**, 032801 (2008)

60. A. Gezerlis, J. Carlson, *Phys. Rev. C* **81**, 025803 (2010)
61. J. Margueron, H. Sagawa, K. Hagino, *Phys. Rev. C* **76**, 064316 (2007)
62. F. Isaule, H.F. Arellano, A. Rios, *Phys. Rev. C* **94**, 034004 (2016)
63. M. Stein, A. Sedrakian, X.G. Huang, J.W. Clark, *Phys. Rev. C* **90**, 065804 (2014)
64. V.A. Khodel, J.W. Clark, V.R. Shaginyan, M.V. Zverev, *Phys. Atomic Nucl.* **77**, 1145 (2014)
65. M. Randeria, E. Taylor, *Ann. Rev. Condens. Matter Phys.* **5**(1), 209 (2014). <http://dx.doi.org/10.1146/annurev-conmatphys-031113-133829>
66. M. Stein, A. Sedrakian, X.G. Huang, J.W. Clark, *Phys. Rev. C* **93**, 015802 (2016)
67. A.D. Jackson, E. Krotscheck, D. Meltzer, R.A. Smith, *Nucl. Phys. A* **386**, 125 (1982)
68. J.M.C. Chen, J.W. Clark, E. Krotscheck, R.A. Smith, *Nucl. Phys. A* **451**, 509 (1986)
69. J.W. Clark, C.G. Källman, C.H. Yang, D.A. Chakkalal, *Phys. Lett. B* **61**(4), 331 (1976)
70. J. Wambach, T. Ainsworth, D. Pines, *Nucl. Phys. A* **555**, 128 (1993)
71. H.J. Schulze, J. Cugnon, A. Lejeune, M. Baldo, U. Lombardo, *Phys. Lett. B* **375**, 1–8 (1996)
72. S. Fantoni, S. Rosati, *Nuovo Cimento* **43A**, 413 (1977)
73. R.B. Wiringa, V.R. Pandharipande, *Nucl. Phys. A* **299**, 1 (1978)
74. V.R. Pandharipande, R.B. Wiringa, *Rev. Mod. Phys.* **51**(4), 821 (1979)
75. E. Krotscheck, *Nucl. Phys. A* **482**, 617 (1988)